AJNR

The Evolution of Cerebral Blood Flow in the Developing Brain: Evaluation with Iodine-123 Iodoamphetamine SPECT and Correlation with MR Imaging

Aya M. Tokumaru, A. James Barkovich, Toshihiro O'uchi, Takeshi Matsuo and Shouichi Kusano

AJNR Am J Neuroradiol 1999, 20 (5) 845-852
http://www.ajnr.org/content/20/5/845

AJNR Am J Neuroradiol 20:845–852, May 1999

The Evolution of Cerebral Blood Flow in the Developing Brain: Evaluation with Iodine-123 Iodoamphetamine SPECT and Correlation with MR Imaging

Aya M. Tokumaru, A. James Barkovich, Toshihiro O'uchi, Takeshi Matsuo, and Shouichi Kusano

BACKGROUND AND PURPOSE: **Although it is well established that brain maturation correlates temporally with the functions the newborn or infant performs at various stages of development, the precise relationship between function and anatomic brain maturation remains unclear. The purpose of this study was to investigate the developmental changes of regional cerebral blood flow (rCBF) in infants and children using iodine-123 iodoamphetamine (^{123}I-IMP) and single-photon emission computed tomography (SPECT). These findings were correlated with the MR imaging appearance of the brain and with known developmental changes.**

METHODS: **Twenty-one ^{123}I-IMP SPECT examinations of 17 patients, ranging in age from neonates to 2 years, were reviewed retrospectively. All children had had transient neurologic events in the neonatal period that did not significantly affect subsequent neuropsychological development. MR studies were performed in 12 of these patients and the MR findings were correlated with the SPECT results.**

RESULTS: **SPECT studies showed a consistent pattern of evolving changes in ^{123}I-IMP uptake, most likely reflecting evolution of rCBF. From the 34th postconceptional week until the end of the second month after term delivery, there was predominant uptake in the thalami, brain stem, and paleocerebellum, with relatively less cortical activity. Radionuclide uptake in both the perirolandic and occipital cortices was well seen around the 40th postconceptional week and increased rapidly thereafter, with a predominance of parietal activity. By 3 months, radionuclide uptake in the cerebellar hemispheres and parietofrontal cortices increased. Frontal and temporal activity increased by age 6 to 8 months. Uptake in the basal ganglia increased by 8 months. By the beginning of the second year, rCBF showed a similar topographic pattern to that in adults.**

CONCLUSION: **The time course of the changes in ^{123}I-IMP uptake in the developing brain as detected by SPECT is similar to that of myelination and most likely reflects an overall topologic maturational pattern of the brain.**

The brain matures in a precisely organized, predetermined pattern (1–3). Although it is well established that brain maturation correlates temporally with the functions the newborn or infant performs at various stages of development, the precise relationship between function and anatomic brain maturation remains unclear. There are several potential approaches to studying the maturation of the brain: among those that have been performed in various animal models are measurements of regional glucose consumption (local cerebral metabolic rates for glucose) and measurements of regional cerebral blood flow (rCBF) (4–9). These studies have established some important concepts in the understanding of brain function during maturation. An understanding of normal brain maturation as assessed by imaging techniques is of vital importance to neuroradiologists, as a study of the immature brain can only be properly interpreted in relation to normal developmental patterns.

In this study, we used iodine-123 iodoamphetamine (^{123}I-IMP) single-photon emission computed tomography (SPECT) to assess the evolution of rCBF in the brains of neonates, infants, and young children who, despite early difficulties, had normal

Received September 5, 1995; accepted after revision January 20, 1999.

From the Department of Radiology, National Defense Medical College, Tokorozawa City, Saitama-Ken, Japan (A.M.T., S.K.); the Department of Neuroradiology, University of California, San Francisco (A.J.B.); and the Department of Radiology, Kameda Medical Center, Kamogawa City, Chiba-Ken, Japan (T.O., T.M.).

Address reprint requests to Aya M.Tokumaru, MD, Department of Radiology, National Defense Medical College, 3–2 Namiki, Tokorozawa City, Saitama-Ken 359-8513, Japan.

Summary of 17 patients examined with ^{123}I-IMP SPECT to study developmental changes in rCBF

Case	Sex/Age at Time of rCBF Study	Age at Time of MR Study	Clinical Information	Laboratory Data	Premedication
1	M/34 w		Low birth weight (1480 g), Apgar scores 4 at 1 min, perinatal convulsion, no developmental delay at 1 y	EEG: normal	Phenobarbituate 0.02 mL/kg
	f/u 38 w				Phenobarbituate 0.02 mL/kg
2	M/35 w	36 w	Low birth weight (1520 g), Apgar scores 4 at 1 min and 7 at 5 min, no neurologic defecit at 6 mo	EEG: normal; MR: no abnormality	Phenobarbituate 0.02 mL/kg
3	M/39 w		Low birth weight (1370 g) Apgar scores 3 at 1 min and 7 at 5 min, no development delay at 2 y	EEG: normal	Phenobarbituate 0.02 mL/kg
4	F/40 w		Low birth weight (1484 g), convulsion at 1 d, Apgar score 4 at 1 min, no developmental delay at 6 mo	CPK: 1580	Phenobarbituate 0.02 mL/kg
5	M/40 w		Low birth weight (1384 g)	MR: normal	Triclofos sodium 30 mg/kg
	f/u 4 mo		No neurologic defecit	MR: normal	Triclofos sodium 30 mg/kg
6	M/40 w	38 w	Hypoglycemia (28 mg/dL)	EEG: normal; MR: normal	Phenobarbituate 0.02 mL/kg
	f/u 53 w		No developmental delay		Triclofos sodium 30 mg/kg
7	M/41 w		Low birth weight, clonic seizure	EEG: normal	Phenobarbituate 0.02 mL/kg
	f/u 4 mo	4 mo	No neurologic defecit	MR: normal	Triclofos sodium 30 mg/kg
8	M/42 w	43 w	Low birth weight (976 g), mild respiratory distress	MR: normal	Triclofos sodium 30 mg/kg
9	M/44 w	42 w	Hypoglycemia at birth (0 mg/dL)	MR: normal; hypopituitarism	Triclofos sodium 30 mg/kg
10	M/5 mo	5 mo	Mild developmental delay suspected at 4 mo	MR: thin subdural effusion	Triclofos sodium 30 mg/kg
		7 mo	No neurologic defecit	MR: normal	Triclofos sodium 30 mg/kg
11	M/6 mo	5 mo	Purulent meningitis, no neurologic defecit at 2 y	MR: meningeal enhancement	Triclofos sodium 30 mg/kg
12	M/8 mo	8 mo	Convulsive attack	MR: temporal arachnoid cyst	Triclofos sodium 30 mg/kg
13	F/10 mo		Convulsive attack		Triclofos sodium 30 mg/kg
14	M/11 mo	11 mo	Faint attack	MR: normal	Triclofos sodium 40 mg/kg
15	M/27 mo		Purulent meningitis with convulsion, no neurologic defecit at 30 mo	EEG: normal	Triclofos sodium 40 mg/kg
16	M/30 mo	5 mo	Hypopituitarism	Small periventricular hemorrhage	Triclofos sodium 30 mg/kg
		22 mo	Disappearance of pituitary stalk		
		26 mo	Atrophy of pituitary gland		
17	M/34 mo	3 y	Atrophy of pituitary gland		Triclofos sodium 40 mg/kg

Note.—^{123}I-IMP indicates iodine-123 iodoamphetamine; rCBF, regional cerebral blood flow; f/u, follow up; CKP, creatine phosphokinase.

clinical development and neurologic outcome. We describe the patterns of radionuclide uptake at sequential stages of development and discuss the meaning of the evolving pattern and its correlation with patterns of myelination.

Methods

^{123}I-IMP SPECT studies of 17 subjects (21 examinations) were reviewed retrospectively. MR imaging studies were available in 12 of the patients (16 examinations) and were correlated with the SPECT studies when possible. The ^{123}I-IMP

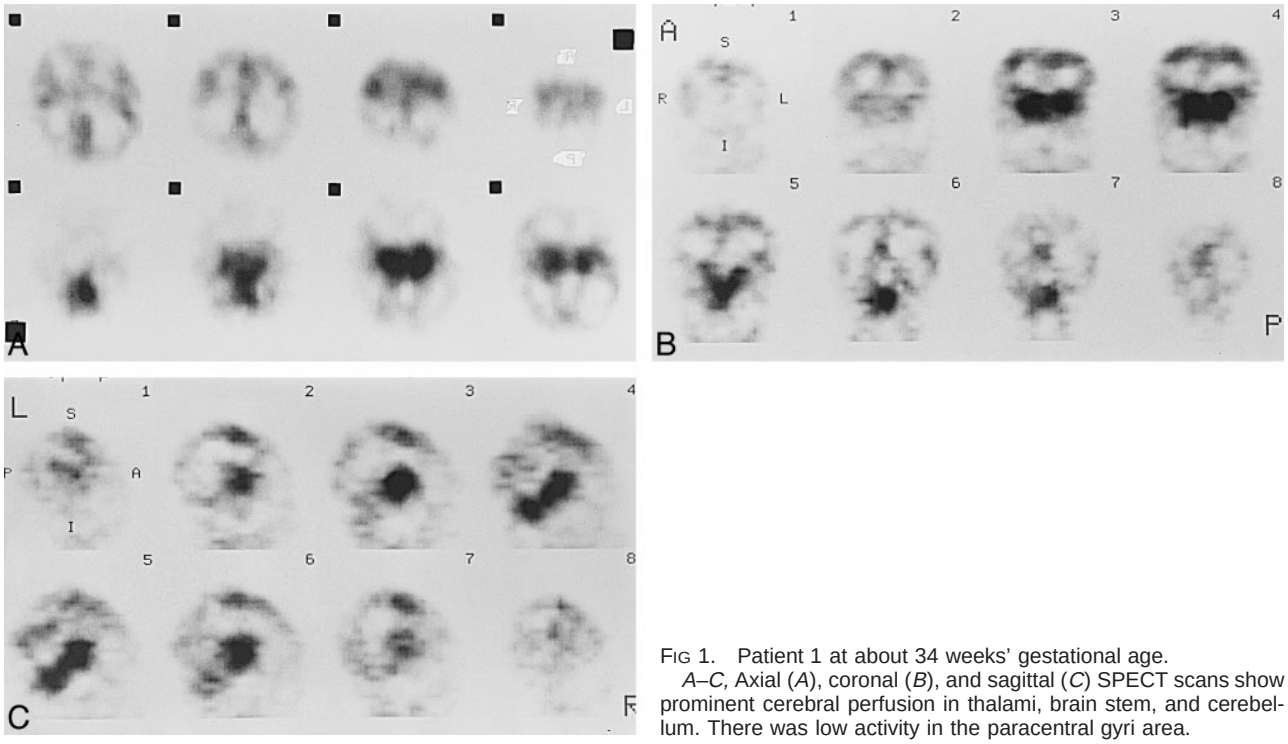

FIG 1. Patient 1 at about 34 weeks' gestational age.
A–C, Axial (*A*), coronal (*B*), and sagittal (*C*) SPECT scans show prominent cerebral perfusion in thalami, brain stem, and cerebellum. There was low activity in the paracentral gyri area.

SPECT studies were performed and the patients selected according to a protocol approved by the local committee for medical ethics at the Universities of Brussels (10). Informed consent was obtained in all cases. Inclusion criteria for neonates were birth weight less than 1500 g, neonatal distress (defined as an Apgar score of less than 4 points at 5 minutes), or perinatal hypoglycemia (serum glucose less than 30 mg/dL). The inclusion criteria for patients older than 5 months were epilepsy or seizures. Each patient had had a transient neurologic event that did not cause subsequent abnormalities on MR images or abnormalities in development, clinical neurologic examination, or EEG at the age of 2 years. The nine patients enrolled as neonates ranged in gestational age from 34 to 44 weeks at the time of their initial SPECT study (nine examinations in neonates). Four of these patients and eight other patients had ^{123}I-IMP SPECT examinations at ages ranging from 2 to 34 months (a total of 12 examinations in infants and young children). The clinical information and ages of the various patients at the time of their imaging studies are compiled in the Table.

For the SPECT studies, 0.05 mCi/kg of high-purity ^{123}I-IMP was administered intravenously using a standard technique. Premedication (see Table) was used in the patients for adequate sedation. SPECT imaging was performed 30 minutes after intravenous administration of ^{123}I-IMP. Using a rotating gamma camera interfaced with a dedicated computer system and a low-energy high-resolution collimator during a 360° rotation, 60 frames were collected with a 64 × 64 matrix. Axial, coronal, and sagittal reconstructions were calculated by filtered back projection using a Butterworth filter after high-frequency cut-off. Sections were 3 pixels (1.2 cm) thick. Data analysis was not quantitative but qualitative, based on visual inspection of the images. The calculated data were estimated by each region of interest/entire brain ratio.

MR examinations were performed at 1.5 T. MR imaging parameters included a 256 × 256 matrix and 4- to 6-mm-thick sections (with a 1- to 2-mm intersection gap). Axial spin-echo (SE) 2500–3000/15,90–120/1 (TR/TE/excitations), and coronal SE 600/15/1 images were obtained in 21 patients. Sagittal SE 600/15/1 images were obtained in 15 patients.

Results

The ^{123}I-IMP SPECT studies revealed a pattern of evolving changes in radionuclide uptake. At around 34 weeks' gestational age, there was prominent uptake in the thalami, brain stem, and central portion of the cerebellum (Fig 1). There was low activity in the paracentral gyri (primary sensorimotor area). At a gestational age of approximately 40 weeks, there was prominent cortical activity in the paracentral gyri and low activity in the occipital cortices (Fig 2). Activity in the thalami, brain stem, and cerebellum showed a similar pattern to that in the preterm infant. By a gestational age of approximately 44 weeks, parietal and occipital activity was more prominent than that of the 40-week neonate (Fig 3). By age 3 months, activity appeared in the frontal and temporal cortices but was still lower than that in the parietal and occipital cortices. Activity in the basal ganglia and cerebellar hemisphere also appeared at this stage (Fig 4). By age 5 months, diffuse cortical activity was recognized, with predominant activity in the parietal cortex (Fig 5). Relative activity in the thalami, brain stem, and cerebellum subsided around this stage. At 8 months of age, activity in the frontal and temporal cortices and basal ganglia was lower still (Fig 6), and by 2 years of age, the pattern of ^{123}I-IMP SPECT uptake (Fig 7) resembled that of adults.

Changes in signal intensity with brain maturation on the MR studies were identical to those described in previous articles (11, 12) (Figs 2, 5, and 7).

Discussion

The results of this study show that changes in ^{123}I-IMP uptake as demonstrated by SPECT par-

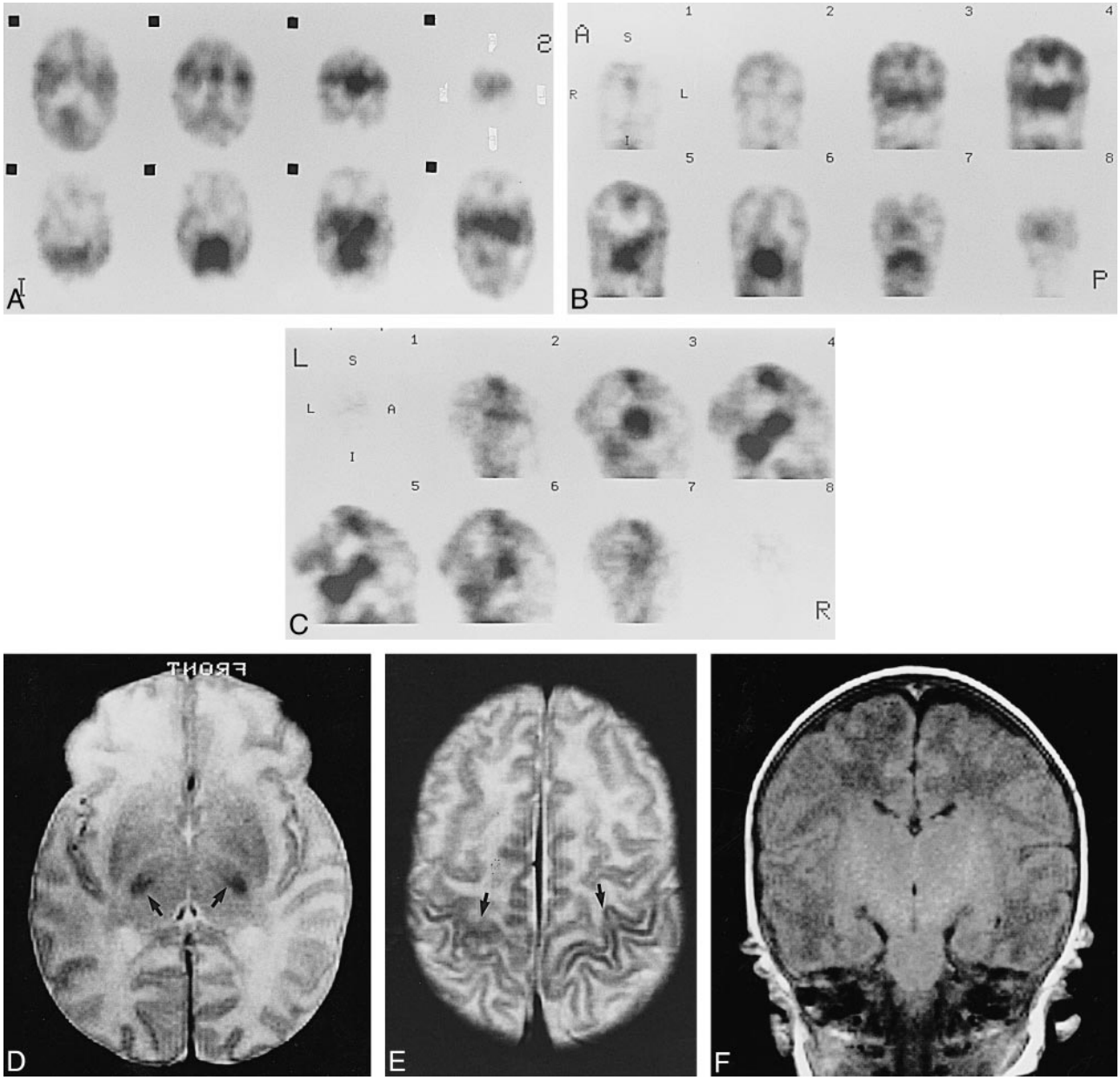

FIG 2. Case 5 at about 40 weeks' gestational age.

A–C, Axial (*A*), coronal (*B*), and sagittal (*C*) SPECT scans show prominent cortical activity in the paracentral gyri and low activity in the medial occipital cortices.

D and *E,* Axial SE (3000/90) MR images show low signal intensity in ventrolateral thalami (*arrows, D*), and paracentral gyri (*arrows, E*), which was considered to be an early myelinated area.

F, Axial SE (600/15) MR image shows high signal intensity in internal capsule to brain stem.

allel, both temporally and topographically, the changes in T1 and T2 relaxation times seen on standard SE MR images. Because the MR changes are attributed to myelination (11, 12), these observations suggest a relationship between myelination and ^{123}I-IMP uptake in the developing brain. As ^{123}I-IMP uptake is generally considered to reflect cerebral perfusion, our findings suggest a relationship between cerebral perfusion and myelination, as initially postulated by von Monakow (13), and with brain maturation in general.

It is well established that rCBF is regulated to meet the requirement of changing cerebral activity (14, 15). Previous investigators, using animal models, have suggested that those cerebral structures with relatively high rCBF or local cerebral metabolic rates for glucose at a specific developmental stage determine the predominant behavioral pattern at that stage (4–9). Our data on the developmental patterns of ^{123}I-IMP uptake in human neonates and children suggest a relationship between increasing perfusion within a neuroanatomic region and the

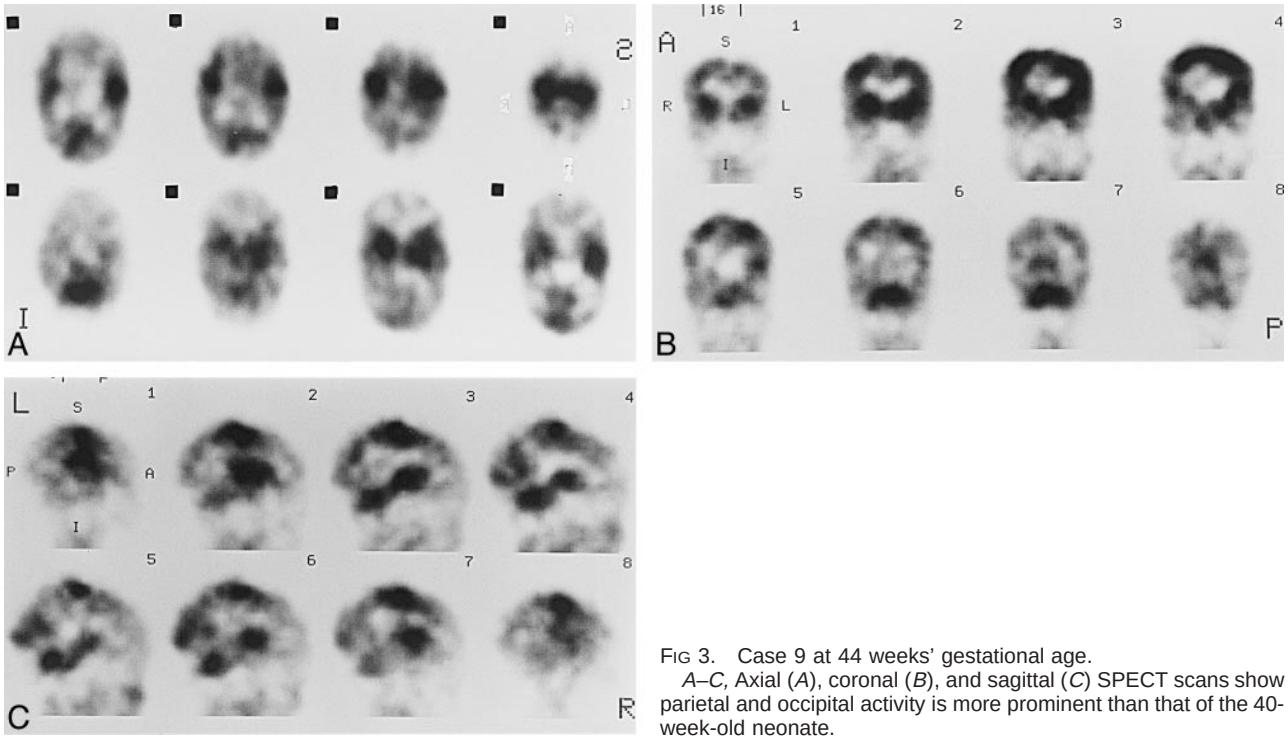

FIG 3. Case 9 at 44 weeks' gestational age.
A–C, Axial (*A*), coronal (*B*), and sagittal (*C*) SPECT scans show parietal and occipital activity is more prominent than that of the 40-week-old neonate.

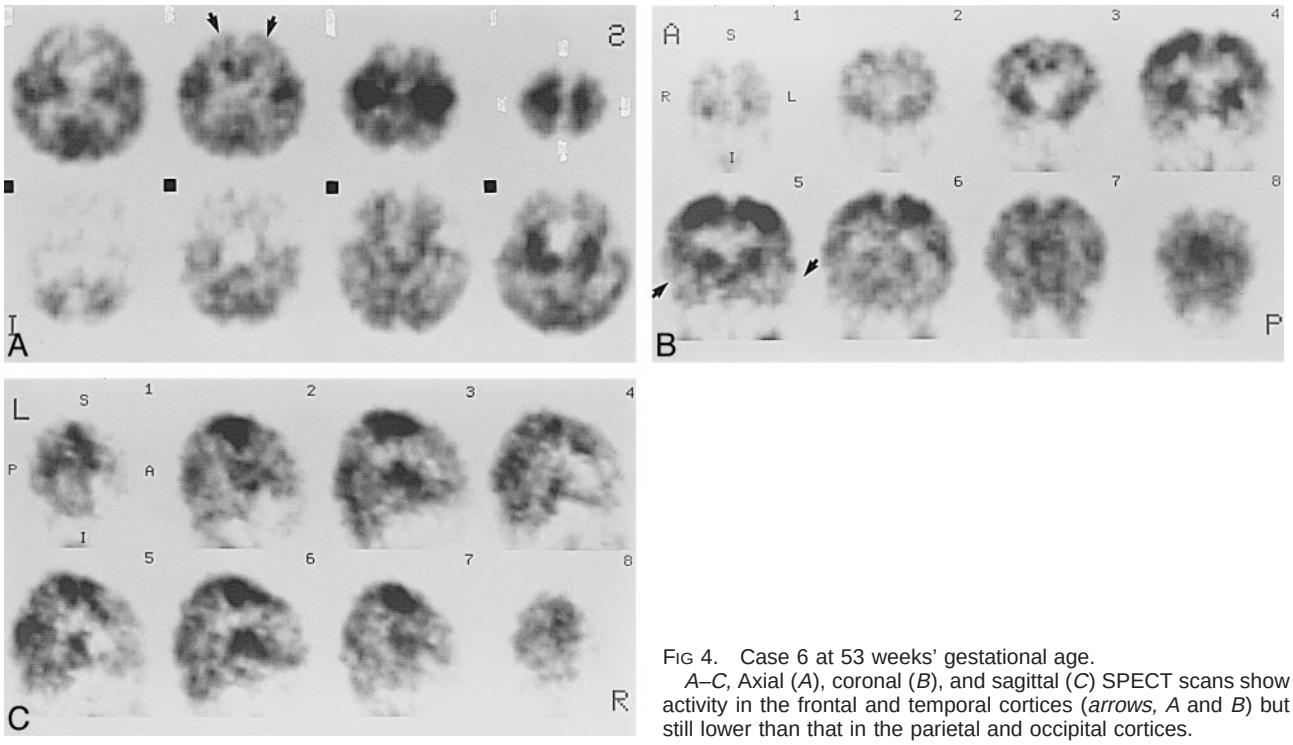

FIG 4. Case 6 at 53 weeks' gestational age.
A–C, Axial (*A*), coronal (*B*), and sagittal (*C*) SPECT scans show activity in the frontal and temporal cortices (*arrows, A* and *B*) but still lower than that in the parietal and occipital cortices.

functional evolution of that structure during infancy. Although the ^{123}I-IMP method is semiquantitative in that it reflects relative, not absolute, rCBF distribution, our data correlate well with the quantitative data of local cerebral metabolic rates for glucose in human neonates obtained by using positron emission tomography (PET) with ^{18}F-fluorodeoxyglucose (FDG-PET) (16).

The developmental changes in the ^{123}I-IMP uptake patterns detected in this study have several potentially interesting implications. The cerebellar uptake noted in the neonates supports other evidence that newborns move extremities and respond to sensory stimuli with primitive responses that involve the function of neocortical areas 4 and 6 and the paleocerebellum (17). The prominent

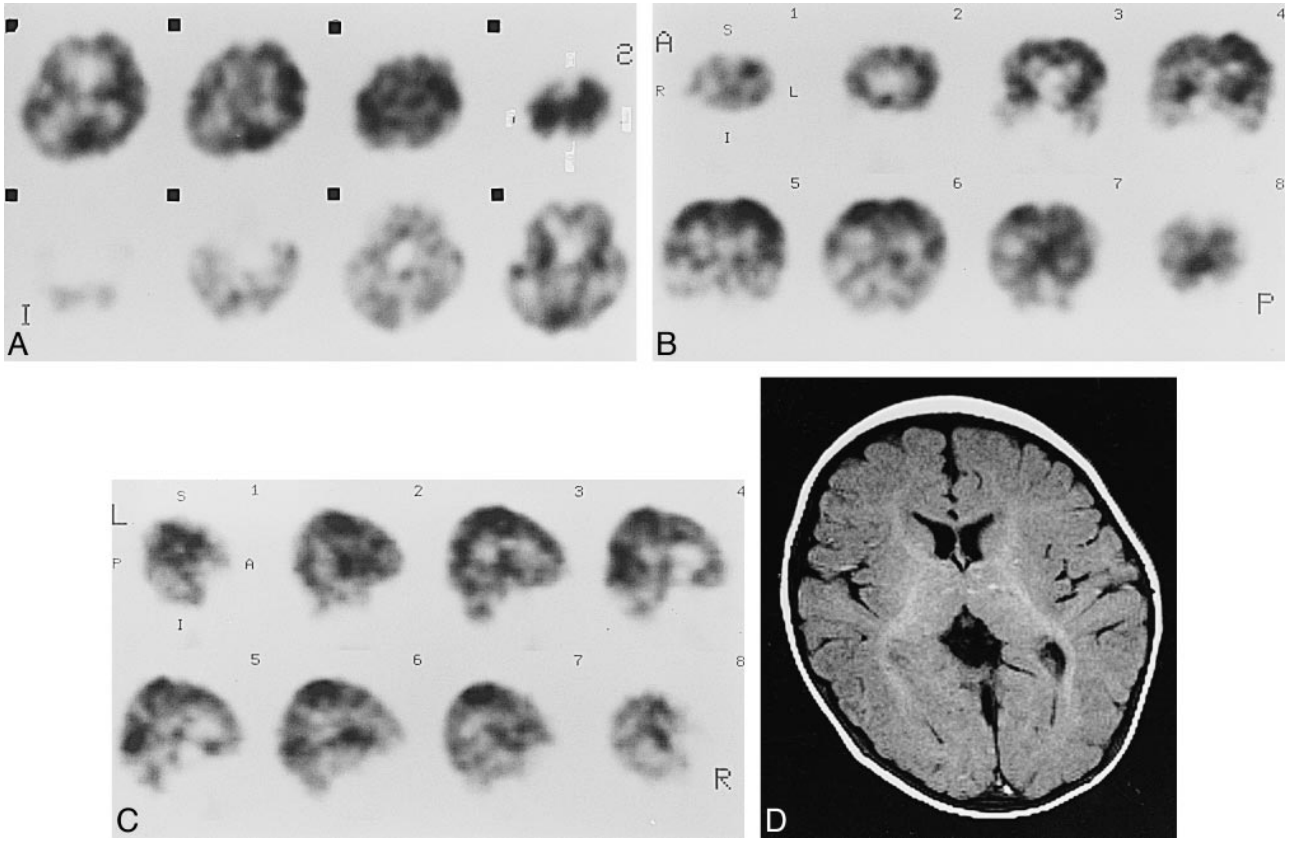

FIG 5. Case 10 at 5 months of age.
A–C, Axial (*A*), coronal (*B*), and sagittal (*C*) SPECT scans show diffuse cortical activity, with prominent activity in parietal cortex. Relative activity in the thalami, brain stem, and cerebellum subsided around this stage.
D, Axial SE (600/15) MR image shows absence of myelination in the frontal white matter.

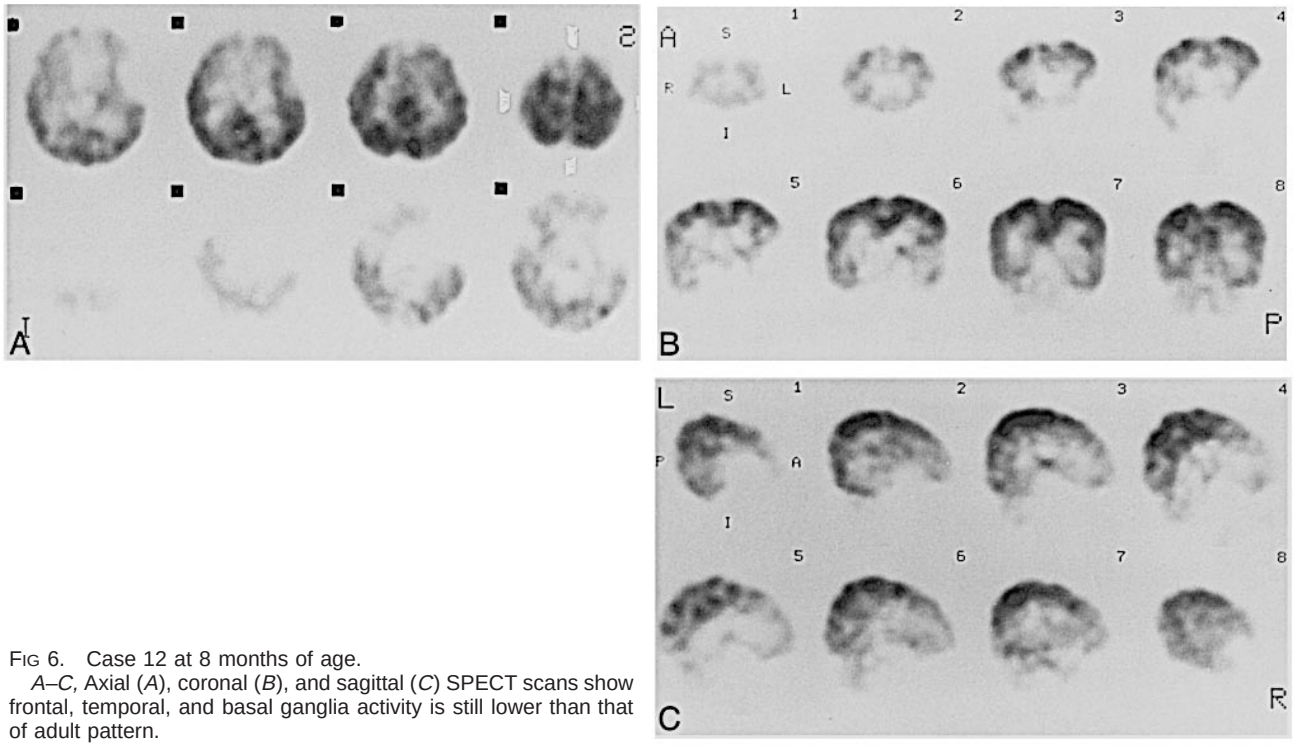

FIG 6. Case 12 at 8 months of age.
A–C, Axial (*A*), coronal (*B*), and sagittal (*C*) SPECT scans show frontal, temporal, and basal ganglia activity is still lower than that of adult pattern.

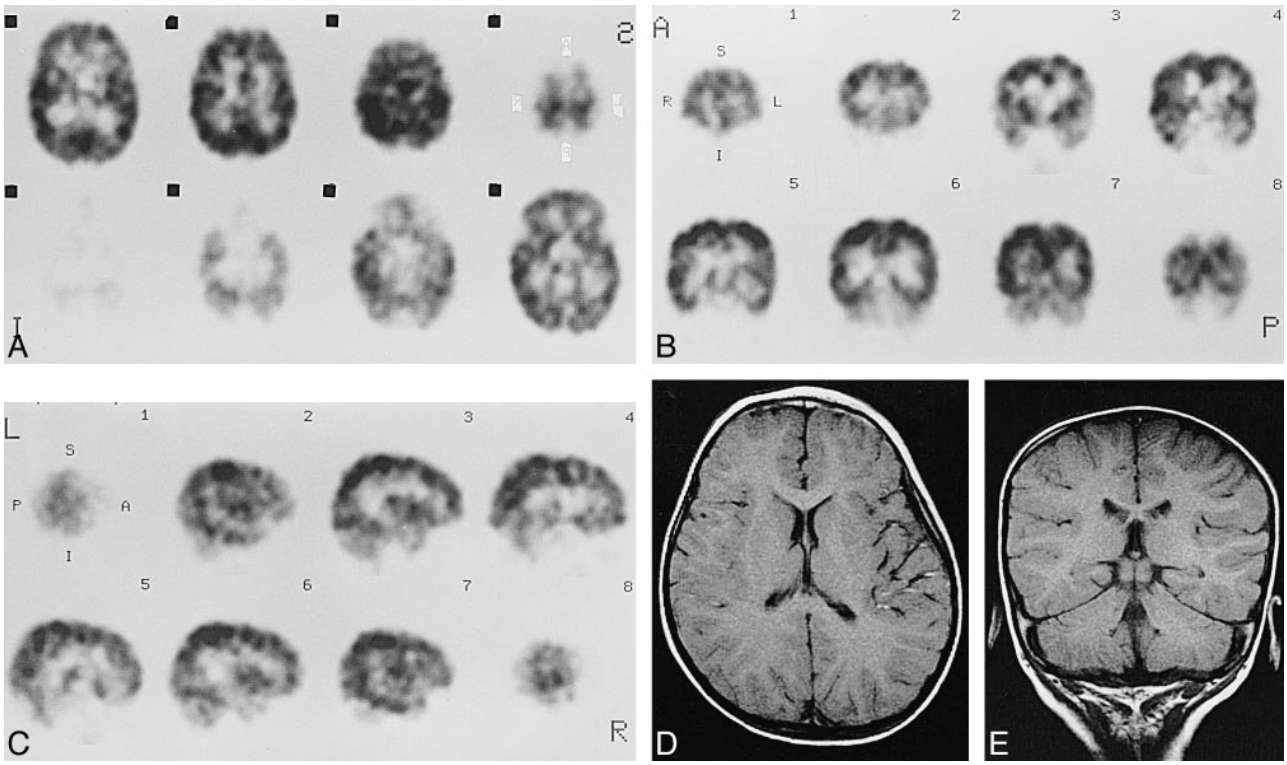

FIG 7. Case 17 at 2 years of age.
A–C, Axial (*A*), coronal (*B*), and sagittal (*C*) SPECT scans show almost similar appearance to adult pattern.
D and *E,* Axial SE (600/15) MR images show myelination in frontal and temporal areas.

rCBF in the neonatal sensorimotor cortex is also consistent with its relatively early morphologic maturation compared with other cortical areas (18). The early uptake of ^{123}I-IMP in the region of the visual cortex is also of interest in that visual cognition develops early and requires high blood flow to the occipital cortex in order to complete the anatomic framework in that area (18). Our observation that ^{123}I-IMP uptake is more prominent in the neonatal thalamus than in the striatum, which has also been observed in animal models (7), suggests relatively greater activity of the thalami in neonates and may reflect the earlier functional maturation of thalamic afferent pathways and their receptor systems. This observation coincides with relatively increased FDG uptake in the thalami of neonates, another manifestation of early thalamic functional maturation (16). A similar metabolic dissociation of thalami and basal ganglia has been recognized in patients with Huntington's chorea on PET studies (19). In this context, it is noteworthy that normal newborn infants manifest physiologic chorealike movements. It is postulated that chorea may be caused by a functional imbalance in the interaction among the striatum, thalamus, and cerebral cortex (16). Pathologic chorea most likely results from loss of striatal function, whereas neonatal physiologic chorea occurs before the emergence of significant activity in the striatum and much of the cerebral cortex.

Our finding of evolution of ^{123}I-IMP uptake and thus rCBF in the neonatal brain also correlates with a developmental evolution in EEG recordings. The EEG, another measure of cerebral cortical activity, also undergoes considerable maturation during the period between 2 and 3 months of age (20). During this time, newborn EEG patterns, such as frontal rhythmic delta and frontal sharp transient waves, disappear and the precursors of alpha rhythms appear. These changes are consistent with our observations of extension of rCBF into the frontal and temporal cortices at this time.

The changing patterns of blood flow in the maturing brain must also reflect to some extent the anatomic evolution of the cerebral vasculature. In mammals, this process appears to be markedly influenced by the functional and metabolic states of the surrounding parenchymal cells. As such cells approach maturity, they command an increasingly rich capillary supply (17).

Our results suggest temporal and spatial relationships between developing patterns of rCBF and myelination in the neonate (1, 11, 12, 21). Although it is difficult to analyze differences between gray and white matter on ^{123}I-IMP SPECT scans and, thus, to compare directly rCBF and myelination, the patterns on the ^{123}I-IMP SPECT scans clearly mirror those attributed to myelin on MR studies (12) and those of local cerebral metabolic rates for glucose on PET scans (16). The relatively high blood flow in myelinating and myelinated ar-

eas of the brain during the perinatal period may reflect the energy demands of the biosynthetic processes associated with myelination (6, 7). In support of this theory, an experimental study measuring blood flow to white matter in the maturing brain noted blood flow in the white matter to be much higher during maturation than at maturity, possibly because of the increased metabolic demands associated with the process of myelination (6). Chugani et al (16) postulated that myelination may be, in part, the cause of the high local cerebral metabolic rates for glucose detected by FDG-PET in the developing brain. They also noted, however, that myelin remodeling is a slow process and therefore seems unlikely to contribute significantly to immediate energy expenditure in the brain. Another possibility is that myelination, rCBF, and local cerebral metabolic rates for glucose are all related to increasing activity in specific regions of the brain that are functionally important during specific developmental periods. The question as to whether increasing function stimulates myelination and blood flow, or whether increased blood flow stimulates myelination and increased activity, or whether all are under genetic control and are turned on simultaneously by the chromosomes is poorly understood and is beyond the scope of this article.

It is known that ^{123}I-IMP binds to an amine binding site in the brain as a delayed distribution (22). In the mature brain, amine binding sites are widespread and numerous, but the distribution of amine binding sites in the neonatal human brain is unknown. This study was based on early images representing a first pass of radionuclide; therefore, it is difficult to determine whether our results are indicative of the sites of amine binding sites in neonates. It is possible, however, that the patterns seen on delayed images might reflect both blood flow and the developmental pattern of amine binding sites. Another possibility is that development of amine binding sites is a component of brain maturation that parallels myelination, increasing local cerebral metabolic rates for glucose, and increasing function. Nonetheless, the fact that local CBF has been shown to increase during white matter maturation by other methods (6) strongly suggests that increased rCBF is an important factor in the patterns we observed.

For ethical reasons, all the children enrolled in this study were selected from a group of patients who were exposed to conditions that might have predisposed them to neurologic dysfunction. At the time of their imaging studies and at later clinical follow up, however, all selected patients had normal neurologic examinations and normal EEG or MR studies. Thus, we believe that the SPECT findings in our patients should be considered normal.

Conclusion

We have demonstrated changing patterns of ^{123}I-IMP uptake in the developing brain that most likely reflect evolution of rCBF. These patterns parallel patterns that have been described previously for myelination on MR images and pathologic examinations and for local cerebral metabolic rates for glucose on PET scans. A knowledge of these evolving normal patterns during development is crucial in the interpretation of these studies in infants and children.

References

1. Yakovlev PE, Lecours AR. **The myelogenetic cycles of regional maturation of the brain.** In: Minkowski A, ed. *Regional Development of the Brain in Early Life.* Philadelphia: Davis; 1967:3–70
2. Flechsig P. ***Anatomie des Menshkichen Gehirns und Ruckenmarks auf myelogenestischer Grundlage.*** Leipzig: Thieme; 1929: 9–37
3. Langworthy O. **Development of behavior patterns and myelination of the nervous system in the human fetus and infant.** *Contrib Embryol* 1933;139:1–57
4. Abrams RM, Ito M, Frisinger JE, et al. **Local cerebral glucose utilization in fetal and neonatal sheep.** *Am J Physiol* 1984;246: R608–R618
5. Cavazzuti M, Duffy TE. **Regulation of local cerebral blood flow in normal and hypoxic newborn dogs.** *Ann Neurol* 1982;11:247–257
6. Kennedy C, Grave GD, Jehle JW, Sokoloff L. **Blood flow to white matter during maturation of the brain.** *Neurology* 1970;20: 613–618
7. Kennedy C, Grave GD, Jehle JW, Sokoloff L. **Changes in blood flow in the component structures of the dog brain during postnatal maturation.** *J Neurochem* 1972;19:2423–2433
8. Kennedy C, Sakurada O, Shinohara M, Miyaoka M. **Local cerebral glucose utilization in the newborn macaque monkey.** *Ann Neurol* 1982;12:333–340
9. Ohata M, Sundaram U, Fredericks WR, et al. **Regional cerebral blood flow during development and aging of the rat brain.** *Brain* 1981;104:319–332
10. Rubinstein M, Denays R, Ham HR, et al. **Functional imaging of brain maturation in humans using iodine-123 iodoamphetamine and SPECT.** *J Nucl Med* 1989;30:1982–1985
11. Holland BA, Haas DK, Norman D, Brant-Zawadzki M, Newton TH. **MRI of normal brain maturation.** *AJNR Am J Neuroradiol* 1986;7:201–208
12. Barkovich AJ. **Normal development of the neonatal and infant brain, skull and spine.** In: *Pediatric Neuroimaging.* 2nd ed. New York: Raven; 1995:9–54
13. Von Monakow, C. **Uber die projections und die Association centrum in Grosshirn.** *Monatwchr Psychiatry* 1900;8:405–420
14. Lassen NA, Ingvar DH, Skinhoj E. **Brain function and blood flow.** *Sci Am* 1978;Oct:62–71
15. Sokoloff L. **Localization of functional activity in the central nervous system by measurement of glucose utilization with radioactive deoxyglucose.** *J Cereb Blood Flow Metab* 1981;1:7–36
16. Chugani HT, Phelps ME, Mazziotta JC. **Positron emission tomography study of human brain functional development.** *Ann Neurol* 1987;22:487–497
17. Craigie EH. **Changes in the vascularity in the brain stem and cerebellum of the albino rat between birth and maturity.** *J Comp Neurol* 1924;38:27–48
18. Rabinowicz T. **The differentiate maturation of the human cerebral cortex.** In: Falkner F, Tanner JM, eds. *Human Growth, 3: Neurobiology and Nutrition.* New York: Plenum; 1979:97–123
19. Kuhl DE, Phelps ME, Markham CH, et al. **Cerebral metabolism and atrophy in Huntington's disease determined by 18-FDG and computed tomographic scan.** *Ann Neurol* 1982;12:425–434
20. Kellaway P. **An orderly approach to visual analysis: parameters of the normal EEG in adults and children.** In: Klass DW, Daly DD, eds. *Current Practice of Clinical Electroencephalography.* New York: Raven; 1979:69–147
21. Fishman MA, Agrawal HC, Alexander A, et al. **Biochemical maturation of human central nervous system myelin.** *J Neurochem* 1975;24:689–694
22. Winshell HS, Horst WD, Braun L, Oldendorf WH, Hattner R, Parker H. **N-isopropyl-(123 I) p-iodoamphetamine: single-pass brain uptake and washout, binding to brain synaptosomes, and localization in dog and monkey brain.** *J Nucl Med* 1980;21:947–952